Available online at www.sciencedirect.com

SciVerse ScienceDirect

Physics Procedia 43 (2013) 337 – 342

Physics Procedia

The 7th International Topical Meeting on Neutron Radiography

Neutron resonance imaging of a Au-In-Cd alloy for the JSNS

M. Ooi[a*], M. Teshigawara[a], T. Kai[a], M. Harada[a], F. Maekawa[a], M. Futakawa[a], E. Hashimoto[a], M. Segawa[a], M. Kureta[a], A. Tremsin[b], T. Kamiyama[c], Y. Kiyanagi[c]*

[a]*Japan Atomic Energy Agency, Tokai-mura Naka-gun Ibaraki 319-1195, Japan*
[b]*Univ. of California, Berkeley, 7 Gauss Way Berkeley, CA 94720-7450, USA*
[c]*Faculty of Eng. Hokkaido Univ, Kita-13 Nishi-8 Kita-ku Sapporo 060-8628, Japan*

Abstract

The Japan Spallation Neutron Source (JSNS) at the Japan Proton Accelerator Research Complex (J-PARC) was developed as a 1-MW spallation neutron source. A Ag-In-Cd alloy was used as the decoupler material in two decoupled moderators. Although the Ag-In-Cd decoupler brings about superior neutronic performance, it has the disadvantage of high residual radioactivity. A Au-In-Cd alloy has been proposed as a solution to this problem. Recently, we successfully produced a ternary Au-In-Cd alloy. The alloy composition was 74.9 at% Au, 0.5 at% In, and 24.6 at% Cd. The distribution of the elements in the alloy was first determined by energy-dispersive X-ray (EDX) analysis. However, it was difficult to measure the In distribution by EDX because the amount of In is very small, and its spectrum is similar to that of Cd. Therefore, pulsed neutron imaging using both a time gated camera system and a multi-channel plate detector was performed to measure the elements in the Au-In-Cd alloy. The analysis was performed at the BL10 in the JSNS on samples of the Au-In-Cd alloy, an In foil, and two Au foils. With this technique, the distribution of Au, In, and Cd in the Au-In-Cd specimen was distinctly determined.

Key words; JSNS, Au-In-Cd alloy, neutron resonance imaging, pulsed neutron.

1. Introduction

A Ag-In-Cd alloy was adopted as the decoupler material in two decoupled moderators of the pulsed neutron source at the Japan Proton Accelerator Research Complex (J-PARC) [1]. A high decoupling energy of 1eV was achieved for the first time in the world in a MW-class spallation neutron source [2-3]. Although the Ag-In-Cd decoupler is superior with respect to neutronic performance, the handling of used moderators is difficult owing to the high residual radioactivity of the decoupler originating from Ag [4]. The moderator life time is assumed to be 30 GWh, which is corresponding to be 20DPA of structural aluminum alloy. To overcome this difficulty, a new alloy, in which Ag in the Ag-In-Cd alloy is replaced with Au, i.e., a Au-In-Cd alloy, was proposed by Harada et al [4]. The radioactivity of a Au-In-Cd decoupler can be reduced to about 1/1000 of that of a Ag-In-Cd decoupler.

Accordingly, an R&D program focused on the production of a Au-In-Cd alloy was launched [5]. As a first step, Au-In-Cd alloy specimens were prepared by melting the three material metal pieces in a small furnace equipped with an infrared heater. The target alloy composition was determined to be 74.9, 0.5, and 24.6 at% for Au, In, and Cd, respectively, in terms of the neutronic performance and burn up of the elements. The elemental distribution of Au and Cd on the surface of an alloy sample was measured by scanning electron microscopy/energy dispersive X-ray

* Corresponding author.
E-mail address: ohi.motoki@jaea.go.jp.

doi:10.1016/j.phpro.2013.03.040

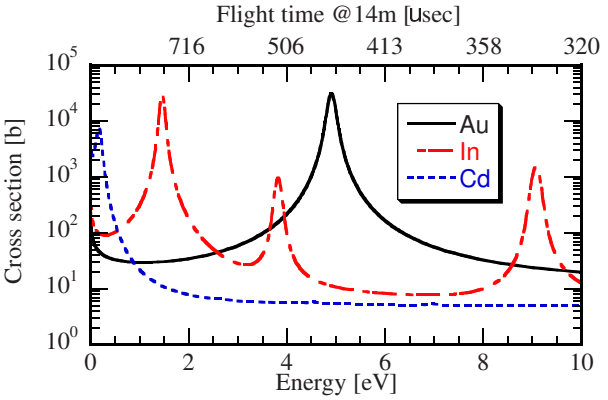

Figure 1. Neutron cross sections of Au, In, and Cd.

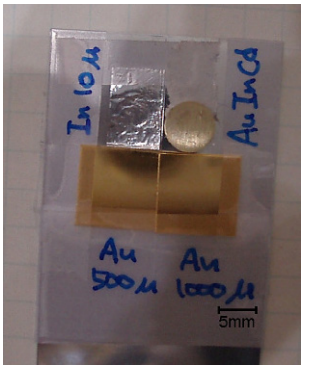

Figure 2. Samples

spectroscopy (SEM-EDX) and was confirmed to be uniform. However, the X-ray peaks for In were overlapped by the X-ray peak for Cd; this is because In content was much smaller than Cd content and the atomic number of In (49) is next to that of Cd (48). Therefore, it was difficult to observe In distribution via SEM-EDX analysis. Consequently, to confirm the uniformity of the alloy including In, a neutron resonance imaging technique was used.

2. Neutron resonance imaging

Most elements have neutron resonance cross sections, such as those shown in Fig. 1 for Au, In, and Cd. Each nuclide has specific neutron resonance energy. For example, in a transmission image of a Au-In-Cd specimen at t = 475 μs, at the neutron resonance peak of Au, the image contributed by the Au content can stand out. Accordingly, we can distinguish certain elements in a sample using neutron resonance imaging based on a time-of-flight imaging technique.

3. Measurement

The imaging experiments were performed at the BL10 (NOBORU) in the JSNS [6]. NOBORU has a beam size of 100 × 100 mm at an L/D ratio of 140. With the rotary collimator, the L/D ratio can be set at 140, 190, 600, or 1875. L/D of 140 was selected in this study. In addition, because of the straight beam line configuration at NOBORU, a very wide energy range from sub-meV to above the keV region can be used.

A Au-In-Cd alloy specimen was cut into a disk sample with thickness 0.9 mm and diameter 6.5 mm. The disk sample was set on a thin Al plate with reference samples, i.e., an In foil (0.01 mm) and two Au foils (0.5 mm and 1 mm), as shown in Fig. 2. The reference samples are used to determine the thickness of the elements in the alloy. The outline of the detector system, which was developed by Kureta et al, can be seen in Fig. 3. The viewing area of this

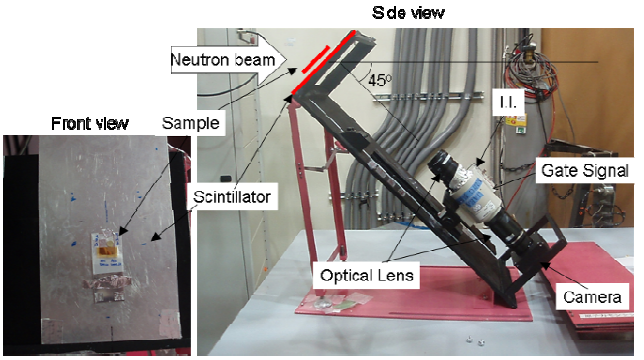

Figure 3. Outline of the camera system.

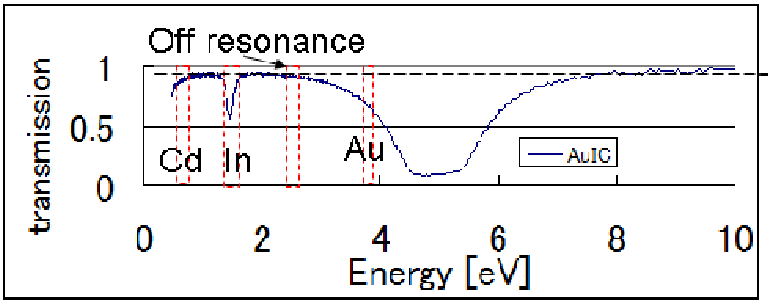

Figure 4. Measured neutron transmission curve of the Au-In-Cd alloy specimen. Doted area indicate measured energy regions for each element.

system can be set to 100 × 100 mm or less. Spatial resolution of this system was about 0.5 mm.

A scintillator plate and a camera system were set at 45° with respect to the neutron beam. Visible light from the scintillator was amplified by the image intensifier (I.I.) and recorded by the camera (Basler A403K). The I.I. was high speed gate type which was manufactured by Hamamatsu Photonics. The I.I was operated in synchronization with the external signals so that it could be used as a shutter for the camera. By using a gate signal to the I.I. with a certain delay from time T0, the image of a certain energy range of interest could be obtained. To obtain clear images, 4000 or 8000 images were accumulated in one measurement.

In order to evaluate the results of the camera system, a B-doped multi-channel plate (MCP) detector was used as the neutron resonance imaging device for the reference measurements [7]. The MCP detector has a viewing area of 14 × 14 mm^2 with a spatial resolution of 55 μm.

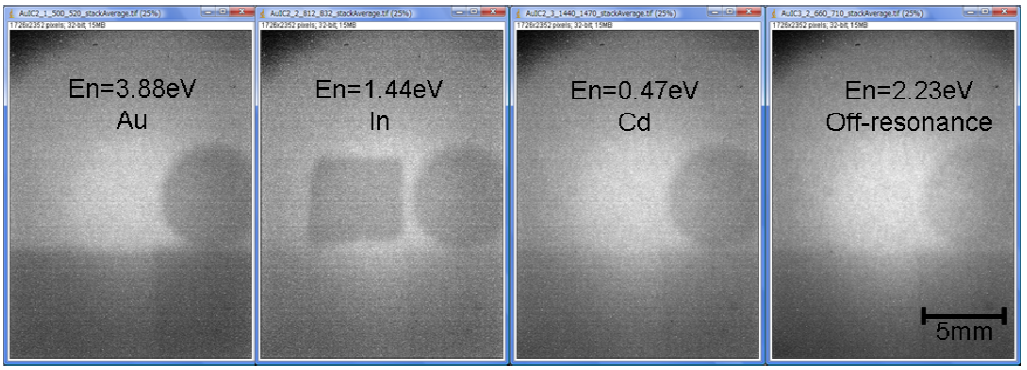

Figure 5. Raw images with the camera system. The neutron energies were 3.88, 1.44, 0.47, and 2.23 eV.

4. Results and discussion

Figure 4 shows the neutron transmission curve of the Au-In-Cd specimen. Figure 5 shows the images obtained with the camera system at En ≈ 3.88 (Au), 1.44 (In), 0.47 (Cd), and 2.23 eV (off-resonance). To avoid non-transmission effect the measured energy for Au was shifted from its peak energy (4.89 eV) to 3.88 eV. Au foils and Au-In-Cd alloy can be seen in all figures of Fig. 5 including the off-resonance energy regions. Because these samples are relatively thick and the macroscopic cross-section values have some finite value even in the off-resonance energy regions. The thickness of the In foil was only 10 μm whereas that of the other samples was greater than 0.5 mm. The estimated neutron transmission in the Au foil (0.5 mm) was 91% whereas that in the In foil was 99.98% at En = 2.23 eV. Therefore, to observe each specific element in the alloy, the off-resonance effect in the images must be eliminated.

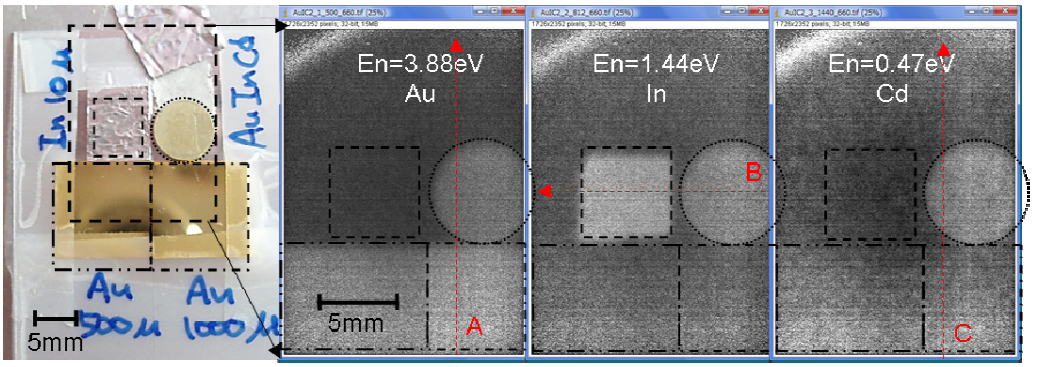

Figure 6. Images of the σ_rNt function for Au, In, and Cd. Dotted lines shows sample area and viewed area.

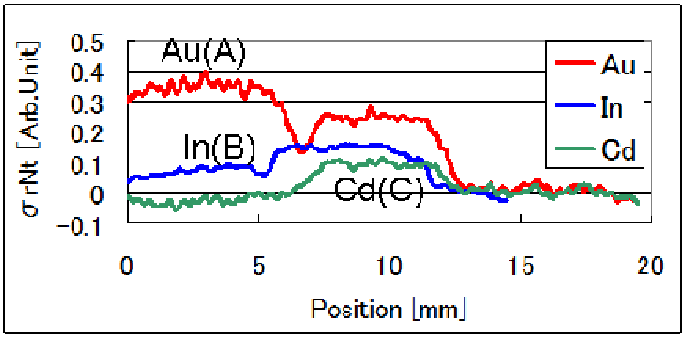

Figure 7. Intensity profiles of Fig. 6. The upper figure shows line A (En = 3.88eV, Au), line B (En = 1.44eV,In), and line C (En = 0.47eV,Cd).

The resonance peak cross-section values of Au and In exceed 10,000 barns. The off-resonance cross-section of the two nuclides is nearly constant at approximately 30 barns. To eliminate the off-resonance effect, the following equations were used:

$$I_r = I_{0r}\exp(-(\sigma_n+\sigma_r)Nt), \quad (1)$$

$$I_n = I_{0n}\exp(-\sigma_n Nt), \quad (2)$$

$$I_{0n}/I_{0r} = C, \quad (3)$$

and

$$-\ln(C\, I_r/I_n) = \sigma_r Nt, \quad (4)$$

where I_r and I_n are the transmitted neutron intensity at the resonance energy and off-resonance energy, respectively; I_{0r} and I_{0n} are the neutron intensity at the resonance energy and off-resonance energy, respectively, without the samples; σ_n is the off-resonance cross section (considered to be nearly constant over the measured energy region); σ_r is the resonance cross section; N is the atomic density; and t is the thickness of the element. C is a correction factor for the neutron intensity and the scintillator efficien
cy that depends on the neutron energy. Eq. (4) can be deduced from Eqs. (1), (2), and (3) to obtain the function of the elemental thickness t.

Figure 6 shows the images of the σ_rNt function for Au, In, and Cd calculated using Eq. (4). The C factor was chosen to make the value consistent in the open beam area. In each sub-figure of Fig. 6, only the target element is seen. Figure 7 shows the intensity profiles along with lines A, B, and C of Fig. 6. The error was approximately 5% in the flat regions. The σ_rNt values of the Au and In samples appear to be correlated to the thickness of the elements. Relative thickness of Au in the alloy was about 0.67mm and that of In in the alloy was 5μm.

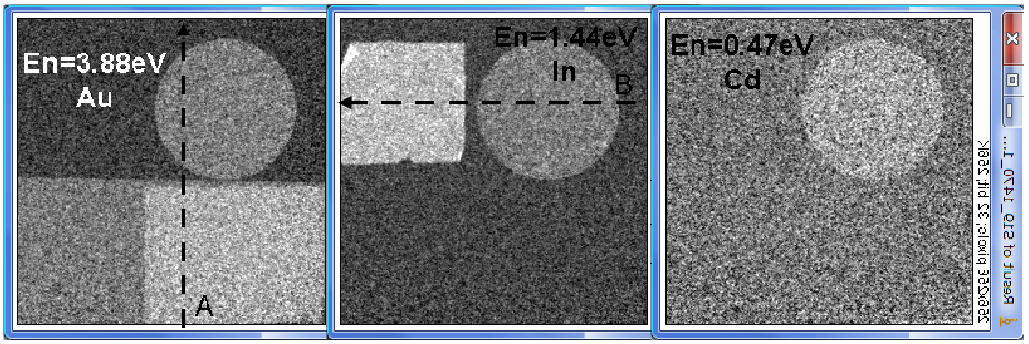

Figure 8. σ_rNt images of the samples measured with the MCP detector. The neutron energies are 3.88 eV (left), 1.44 eV (center), and 0.47 eV (right).

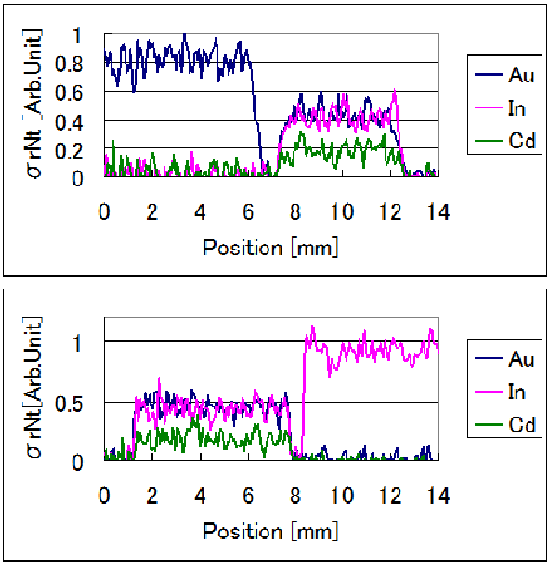

Figure 9. Plot profiles of the images in Fig. 8. The upper figure is for Line A, and the lower figure is for Line B.

To confirm these results, the data obtained with the camera system were compared with the data generated using the MCP detector. Figure 8 shows the results for conversion of the σ_rNt functions measured with the MCP detector. The specific elements in the alloy can also be observed with the MCP detector. In addition, the images confirm that the Au-In-Cd alloy is homogeneous. Furthermore, the clear edge of the samples can be seen in Fig. 8. With the camera system, the sample edges were not clear owing to the resolution of the neutron converter.

Figure 9 shows the profiles of the samples measured using the MCP detector. The same relationship between the σ_rNt values and the thickness of the elements can be seen for the Au and In samples. The value is not the same in Fig.7 and Fig. 9, because of the background is different for each method and it was not corrected here. In the figure 4, transmission curve should be zero around 5eV but it is not zero due to the background such as gamma ray or scattering neutrons.

The Au thickness in the Au-In-Cd alloy specimen was estimated from the composition of the alloy, was approximately 0.67 mm. However, the σ_rNt value for Au in the alloy was nearly half that of the Au foil (1 mm). This result indicates that elemental thickness in the alloy was underestimated by this method. On the other hands, estimated thickness of In in the alloy was 5 μm, it is half of the thickness of the In foil. The measured results show the same thickness ratio.

With these methods, we can see the specific element in the alloy. However, evaluated thickness of the element was not comparable for each detector system. It is required to improve the analytical method to correct the background.

5. Summary

The neutron resonance imaging of a Au-In-Cd alloy specimen was performed in the J-PARC/MLF. The distribution of Au, In, and Cd in the alloy was illustrated individually, and we confirmed that each element in the alloy was mixed uniformly. By comparing the alloy to pure metal foils, the thickness of each element in the alloy was roughly evaluated. It is required to improve the analytical method.

There are some issues for spatial resolution and aberration problem in the camera system. However, it is still useful for large sample and we are planning to make larger sample and utilize this technique to the production of the moderators.

References

[1] Y. Ikeda, Nucl. Instr. and Meth. A 600 (2009) 1.
[2] M. Teshigawara, et al., J. of Nucl. Mat. 343 (2005) 154.
[3] M. Teshigawara, M. Harada et.al., J. of Nucl. Mat 356 (2006) 300.
[4] M. Harada, M. Teshigawara, F. Maekawa, M. Futakawa, J. of Nucl. Mat. 398 (2010) 93.
[5] M. Ooi, M. Teshigawara et.al., J. of Nucl. Mat. 431 (2012) 218
[6] K. Oikawa, et al., Nucl. Instr. Meth. A 589 (2008) 310.
[7] A.S.Tremsin, J.B. Mcphate, J.V. Vallerga, et. al., Nucl. Instr. Meth. A 604 (2009) 140.